Serial Section-Based 3D Reconstruction of *Anaxagorea* (Annonaceae) Carpel Vasculature and Implications on Integrated Axial-Foliar Origin of Angiosperm Carpels

Ya Li,[1,†] Wei Du,[1,†] Ye Chen,[2] Shuai Wang,[3] Xiao-Fan Wang[1,*]

1 College of Life Sciences, Wuhan University, Wuhan 430072, China

2 Department of Environmental Art Design, Tianjin Arts and Crafts Vocational College, Tianjin 300250, China

3 College of Life Sciences and Environment, Hengyang Normal University, Hengyang 421001, China

*Author for correspondence. E-mail: wangxf@whu.edu.cn

† These authors have contributed equally to this work

Running Title: Integrated Axial-Foliar Carpel Origin

Abstract

The carpel is the basic unit of the gynoecium in angiosperms and one of the most important morphological features distinguishing angiosperms from gymnosperms; therefore, carpel origin is of great significance in angiosperm phylogenetic origin. Recent consensus favors the interpretation that the carpel originates from the fusion of an ovule-bearing axis and the phyllome that subtends it. It has been confirmed by morphological and molecular evidence that foliar homologs are involved in carpel evolution. Consequently, if axial homologs can be traced in the carpel, it would more likely be derived from an integrated axial-foliar structure. This study aimed to reveal the axial structures in carpels by analyzing the continuous changes in vasculature from the receptacle to the carpels and ovules. *Anaxagorea* is the most basal genus in a primitive angiosperm family, Annonaceae. The conspicuous carpel stipe at the base of each carpel makes it an ideal material for exploring the possible axial homologous structure in the carpel. In this study, floral organogenesis and the topological vasculature structure were delineated in *Anaxagorea luzonensis* and *Anaxagorea javanica*, and a 3D-model of the carpel vasculature was reconstructed based on the serial sections. The results show that (1) at the flowering stage, the number of vascular bundles entering each *Anaxagorea* carpel from the receptacle was significantly higher than three, arranged in a radiosymmetric pattern, and forming a basal ring at the base of each carpel. (2) All carpel bundles were only connected with the central stele. (3) At the slightly upper part of the carpel, all lateral bundles from the basal ring were reorganized into two groups, each forming a lateral bundle complex below the respective placenta. Bundles in each lateral bundle complex were also ringed. (4) The ovule bundles were composed of non-adjacent bundles in the lateral bundle complex. The results of the present study suggest that the circular arrangement of bundles in the receptacle, carpel stipe, and placenta of *Anaxagorea* are in line with the composite axial-foliar nature of the carpel, and provide a morphological basis for further research on the origin of the carpel.

Key words: 3D reconstruction; *Anaxagorea*; angiosperms; organogenesis; origin of the carpel; vascular anatomy

INTRODUCTION

Since Darwin's time, the elucidation of angiosperm origin and its evolutionary success has been a primary goal of plant science (Kennedy and Norman, 2005). The term "angiosperm" is derived from the Greek words angeion, meaning "container," and sperma, meaning "seed." Therefore, the carpel, an angiosperm-specific "seed container", is the definitive characteristic of angiosperms. The carpel is the basic unit of the gynoecium; it protectively surrounds the ovules by enclosing and sealing off their rims or flanks (Dunal, 1817; Robinson-Beers, 1992; Endress, 2015). The evolution of the carpel sets angiosperms apart from other seed plants, which develop exposed ovules. Previous studies have attempted to identify the potential angiosperm ancestors through phylogenetic analyses based on fossil, morphological, and molecular data. In these studies, particular emphasis was placed on assessing which ovule-bearing structures of various seed plants could be transformed into carpels. However, due to early differentiation, the extant angiosperms and gymnosperms underwent a long independent evolutionary process that resulted in the reproductive structure of the basal angiosperms and extant gymnosperms being significantly different, although some species of the two groups may have undergone convergent evolution (Winter et al., 1999; Soltis et al., 2002; Magallon et al., 2015). As a result, the origin of the carpel has not been solved.

The origin of the carpel is considered either a conduplicate leaf-like structure bearing marginal ovules, or an integration of the ovule-bearing axis and the foliar appendage. Based on developmental evidence and functional genetics studies, more recent consensus favors the latter interpretation (Skinner et al., 2004; Doyle, 2008; Wang, 2010, 2018; Mathews and Kramer, 2012; Liu et al., 2014; Zhang et al., 2017; Zhang et al., 2019). Owing to the difference between the two interpretations, it is important to determine whether the ovule-bearing axis is involved in the evolution of the carpel. Since it has been confirmed that foliar homologs are involved in the evolution of the carpel based on morphological and molecular evidence, if axial homologs can be found in the carpel, it would indicate that the carpel more likely derived from an integrated axial-foliar structure.

In this study, two *Anaxagorea* (Annonaceae) species were selected for floral organogenesis and vascular anatomic examination. Annonaceae represents one of the largest families in the Magnoliales that is one of the most important lineages in the early radiation of angiosperms (Sauquet et al., 2003), while *Anaxagorea* is the most basal genus of Annonaceae (Doyle and le Thomas, 1996; Doyle et al., 2004; Chatrou et al., 2012; Chatrou et al., 2018). *Anaxagorea* carpels are apocarpous (free) throughout their life history (Deroin, 1988), and each has a notably long carpel stipe (Endress and Armstrong, 2011). The aim of this study was to histologically analyze relationships among the receptacle, carpel, and ovule, based on vasculature through continuous anatomical observations and 3D reconstruction, so as to provide a morphological basis for further studies on the carpel axial-foliar origin hypothesis.

MATERIALS AND METHODS

Scanning Electron Microscopy and Paraffin Sectioning

Anaxagorea luzonensis flower samples at different floral stages (from early bud to young fruit) were collected from the Diaoluo Mountain, Hainan, China, in July 2017 and *Anaxagorea javanica* from the Xishuangbanna Tropical Botanical Garden, Yunnan, China in May 2017. The gynoecia were isolated and preserved in 70% formalin-acetic acid-alcohol (5:5:90, v/v), and the fixed specimens were dehydrated in a 50% to 100% alcohol series. To delineate the structure and development of the carpel, carpels were removed from the gynoecia, passed through an iso-pentanol acetate series (SCR, Shanghai, China), critically point-dried, sputter-coated with gold, observed, and photographed under a scanning electron microscope (Tescan VEGA-3-LMU, Brno, Czech Republic). Flowers and carpels were embedded in paraffin, serially sectioned into 10–12-μm thick sections, and stained with Safranin O and Fast Green to illustrate the vasculature. The transverse sections were examined and photographed using a bright-field microscope (Olympus BX-43-U, Tokyo, Japan). In addition, longitudinal hand-cut sections were made and observed for a rough check and better understanding of the vasculature.

Topological Analysis of Carpel Vasculature

Consecutive paraffin sections, 12-μm each, of *A. javanica* were stained with aniline blue, examined and photographed after excitation at 365 nm using an epifluorescence microscope (Olympus BX-43-U, Tokyo, Japan) and a semiconductor refrigeration charged coupled device (RisingCam, MTR3CMOS). Manual image registration of each dataset was arried outusing Photoshop CC 2017 (Adobe, San Jose, CA, US). Forty-five images were selected equidistant from the 423 sections taken for the 3D reconstruction. The figures were organized according to the vascular bundle outlines of the sections by using Photoshop CC 2017 and Illustrator CC 2017 (Adobe). The xylem and phloem contours were manually drawn, extracted as paths with the pen tool, and exported in DWG format. The DWG files were imported into 3Ds Max 2016 (Autodesk, San Rafael, CA, US) and sorted according to the distance and order of the sections. The paths were converted to Editable Spline curves to generate the basic modeling contour. The Loft command of Compound Objects was used to get the shape of the Editable Spline, and a complete 3D carpel vasculature model was generated.

RESULTS

Gynoecium Structure and Carpel Organogenesis

The flowers of two study species were trimerous with a whorl of sepals, two morphologically distinct whorls of petals, and numerous stamens (and inner staminodes of *A. Javanica*) (**Figures 1A–D**).

A. luzonensis usually exhibits two to four completely separate carpels (**Figures 1A, G**). The carpel primordia are almost hemispherically initiated and larger than the stamen primordia (**Figure 1F**). Each carpel consists of a plicate zone, a very short ascidiate zone (**Figures 3G, 5I, J**), and a long, conspicuous stipe (**Figure 2F**). Carpel stipe ontogenesis occurs at the early stages of carpel development (**Figure 2B**). The continuous growth of the flanks on the ventral side of the young carpel triggers its

early closure; however, the closure does not extend to the base of the carpel, where the carpel stipe was previously present (**Figure 2C**). Subsequently, the dorsal region of each carpel thickens markedly, and the stigma forms (**Figures 2D, E**). At anthesis, the carpels are widest at the basal region with an arch on the abaxial side. The carpel stipe remains elongate, accounts for approximately a quarter of the carpel length at anthesis, and continues to elongate during the fruiting stage (**Figure 1F**). Each carpel has two lateral ovules with the placentae at the ovary base (**Figures 3H, 5L**).

A. Javanica exhibits a multicarpellate gynoecium (**Figures 1B, J**). The carpels are completely separate and appear whorled at initiation (**Figure 1I**); as the carpel volume increases, the whorled structure becomes less obvious because the space in floral apex becomes limited. Each carpel consists of a plicate zone and a conspicuous carpel stipe (**Figure 2J**) but lacks the short ascidiate zone. The carpel stipe ontogenesis occurs in the early stages of carpel development (**Figure 2H**) and remains elongate during the flowering and fruiting stages (**Figures 1D, 2I–J**). Each carpel has two lateral ovules.

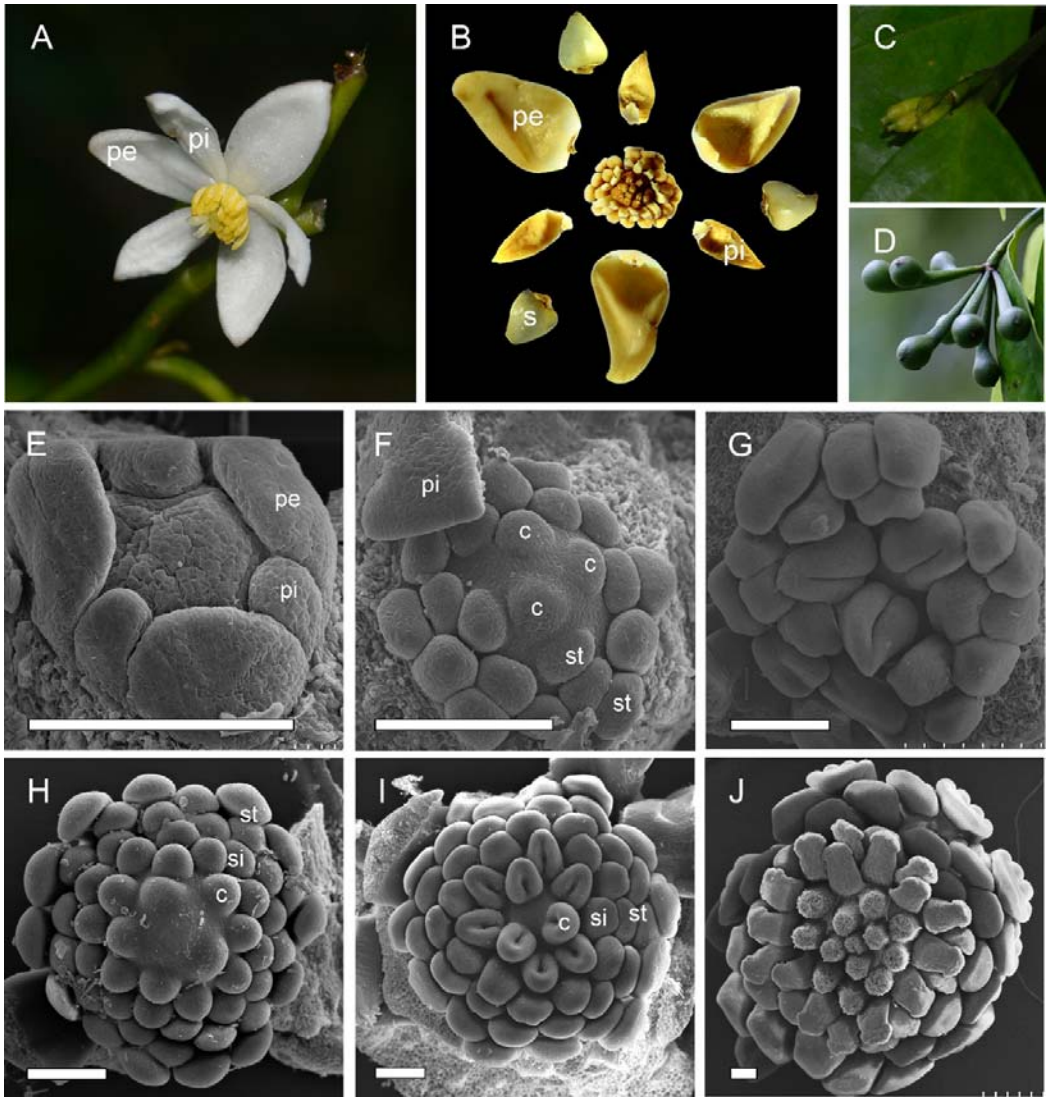

FIGURE 1. Floral morphology and gynoecium development in two *Anaxagorea* species. **(A)** *Anaxagorea luzonensis* flower. **(B)** *Anaxagorea javanica* flower. **(C)** Young *A. luzonensis* fruit. **(D)** Mature *A. javanica* fruit. **(E–G)** *A. luzonensis* floral development. **(H–J)** *A. javanica* gynoecium development. s, sepal; pe, outer petal; pi, inner petal; st, stamen; si, staminode; c, carpel. Scale bars =200 μm.

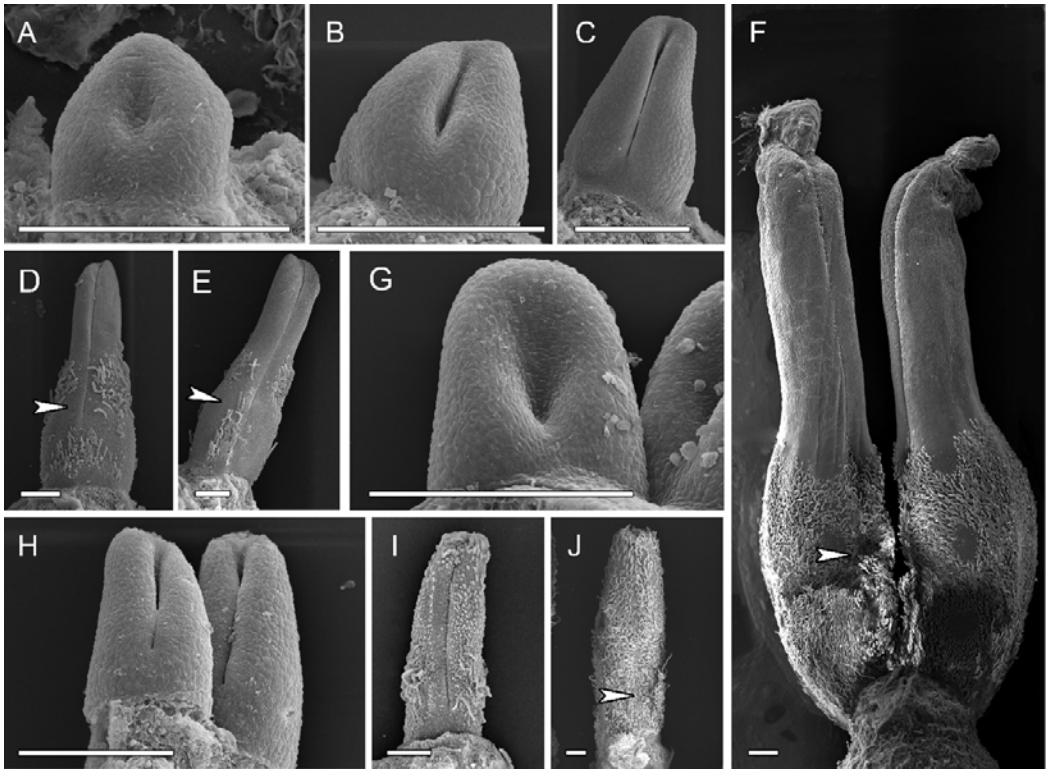

FIGURE 2. Carpel organogenesis in two *Anaxagorea* species. **(A–F)** *Anaxagorea luzonensis*. **(A)** Carpel primordia. **(B–C)** Carpel stipe emergence. **(D–E)** Carpel thickening and stigma formation, showing carpel stipe elongation. **(F)** Mature carpels. **(G–J)** *Anaxagorea javanica* shows similar carpel developmental features to changes depicted in **A–E, F**. Ventral slit end indicated by arrows. Scale bars = 200 μm.

Vasculature from Receptacle to Carpel

In the *A. luzonensis* cross-sections, the receptacle base presented a hexagon of 18 bundles from the pedicel stele (**Figure 3A**). The hexagon had six breaks, which built up a crown of the cortical vascular system to supply the sepals and the two whorls of petals and the stamens (**Figures 3B**). The central stele, composed of 18 bundles, finally broke into two 9-bundle groups at the floral apex and ran into the two-carpel gynoecium (**Figures 3C, D**). Each group of nine bundles assembled as a basal ring around the parenchyma at each carpel base (**Figures 3E**). At the slightly upper part of each carpel, several bundles emerged on the lateral side, and the basal ring broke, from which the dorsal bundle separated and the lateral bundles reorganized into two groups of lateral bundle complexes (**Figures 3F**). In each of the lateral bundle complexes, the adjacent bundles tended to join, assembling into an amphicribral pattern (the xylem surrounded by the phloem) **Figure 3G**. Below each placenta, each of the amphicribral lateral bundle complexes transformed into a set of "C"-shaped lateral bundle complexes, from which the ovule bundles separated, while the other bundles ran into the ovary wall. There were no horizontal connections between the dorsal and other bundles (**Figure 3H**).

The pseudosteles at the base of the *A. Javanica* receptacle were triangular, with ~ 45 bundles. The outer six cortical traces were cylindrical and served the sepals and petals (**Figures 4A, B**). At a slightly higher level, the androecial bundles emerged and served the stamens by repeated branching, and the staminode bundles emerged as a crown around the central stele (**Figure 4C)**. Before entering the gynoecium, the central stele enlarged and broke up into ~ 70 bundles to supply the nine carpels, and each carpel was served by 7–10 bundles (**Figures 4D–E**). The vascular bundle arrangement was similar to ascending sections in *A. luzonensis*, with the basal ring and amphicribral lateral bundle complexes presented in each carpel (**Figures 4F–H**).

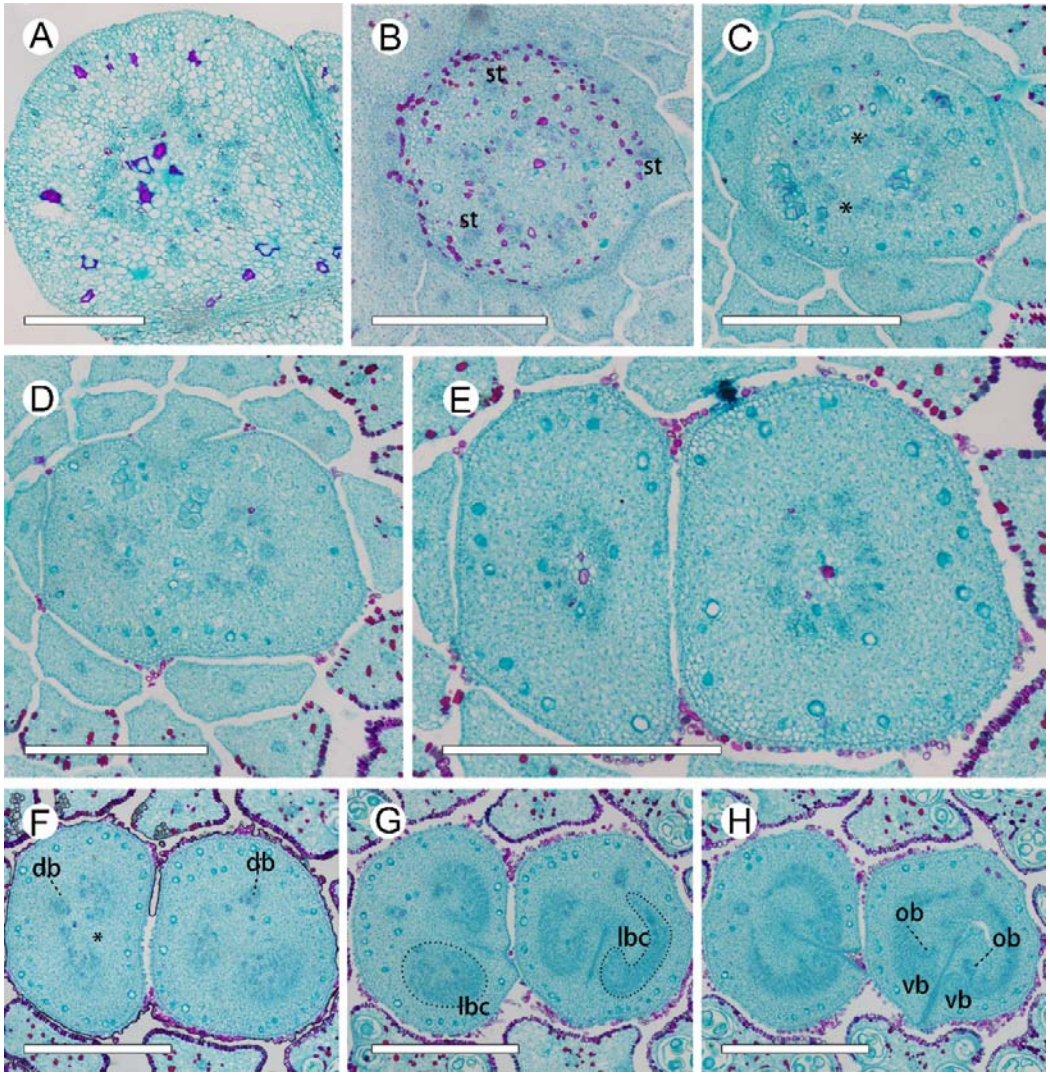

FIGURE 3. Ascending paraffin transections of *Anaxagorea luzonensis* flower. **(A)** Base of receptacle. **(B)** Mid-section of androecia, showing stamen bundles and central stele. **(C)** Top of receptacle, showing central stele divided into two groups (* marked the breaks). **(D)** Bundles from the central stele enter carpels. **(E)** Base of carpels, showing basal ring. **(F)** Upper part of carpel stipes, showing the basal ring breaks (marked as *). **(G)** Bottom of ovary locule, showing amphicribral lateral bundle complexes (left) and "C"-shaped lateral bundle complexes (right). **(H)** Base of ovary locule. st, stamen; db, dorsal bundle; lbc, lateral bundle complex; vb, ventral bundle; ob, ovule bundle. Scale bars = 500 μm.

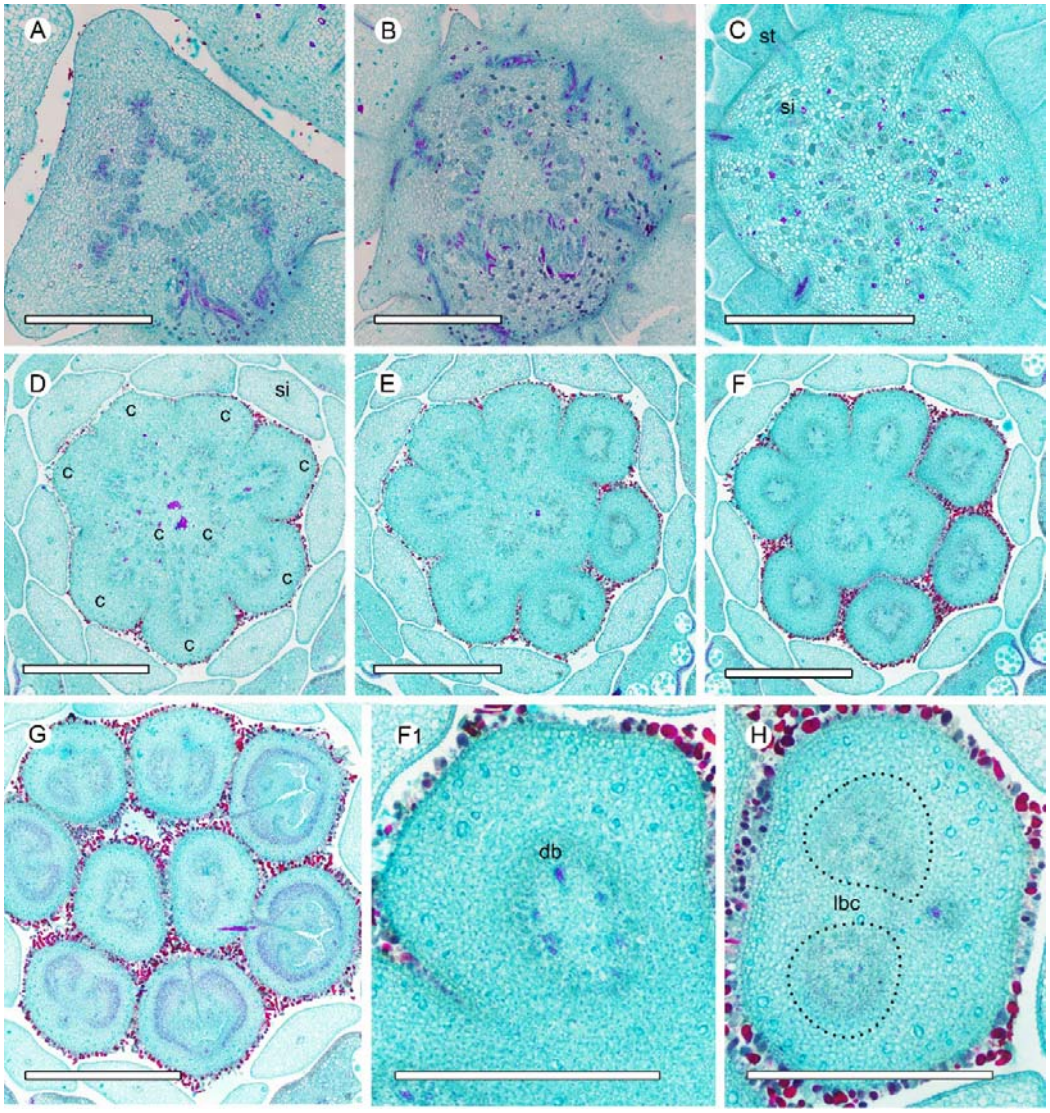

FIGURE 4. Ascending paraffin transections of *Anaxagorea javanica* flower. **(A)** Base of receptacle, showing six groups of vascular bundles and sepal connections. **(B)** Points of petal connection to receptacle, showing perianth bundles. **(C)** Androecial bundles serving stamens by repeated branching. **(D–E)** Base of gynoecium, showing enlarged central stele breaks and bundles distributed into carpels. **(F–G)** Carpel vasculature at different positions. **(F1)** Detailed view of **(F)**, showing basal ring of carpel. **(H)** Amphicribral lateral bundle complexes in carpel. st, stamen; si, staminode; c, carpel; db, dorsal bundle; lbc, lateral bundle complex. Scale bars = 500 μm.

3D-Reconstruction of Carpel Vascular Topology

At the base of a mature *A. luzonensis* carpel, 15 discrete bundles were arranged in a radiosymmetric pattern, forming a basal ring around the central parenchyma (**Figure 5A**). At the slightly upper part, the basal ring curved inward on the ventral side and broke away from the invagination (**Figures 5B, C**). The bundles (except the dorsal) divided into two groups on each side of the carpel, each forming a lateral bundle complex, which was also ring-arranged. At the flowering stage, the lateral bundle complexes corresponded to the above-mentioned sections of the amphicribral complexes (**Figures 5D–F**). Below each placenta, bundles of each lateral bundle complex broke up on the dorsal side and transformed into a "C"-shaped lateral bundle complex (**Figures 5G, H**). The bundles on the ventral side of each lateral bundle complex gathered together (excluding the ventral bundle) and entered each ovule, while other bundles entered into the ovary wall. The ovule bundles were amphicribral. (**Figures 5I–L**).

Consecutive cross-sections of *A. Javanica* were similar in vasculature to those of *A. luzonensis* (**Figures 6A–D**). The base of the mature *A. Javanica* carpel exhibited 16 distinct bundles forming the basal ring (**Figure 6A, F**). The 3D model showed that (1) the basal ring and lateral bundle complex were cylindrical (**Figures 6F, H)**. (2) The ovules were fed directly by bundles from the base of the carpel through the lateral bundle complex. (3) Each ovule bundle was formed from several non-adjacent lateral bundles, and two bundles of them that fed each ovule joined on the ventral side (**Figures 6G, I)**. (4) The dorsal bundle remained independent throughout ontogenesis, without any link to other bundles (for details, please refer to the supplemental data).

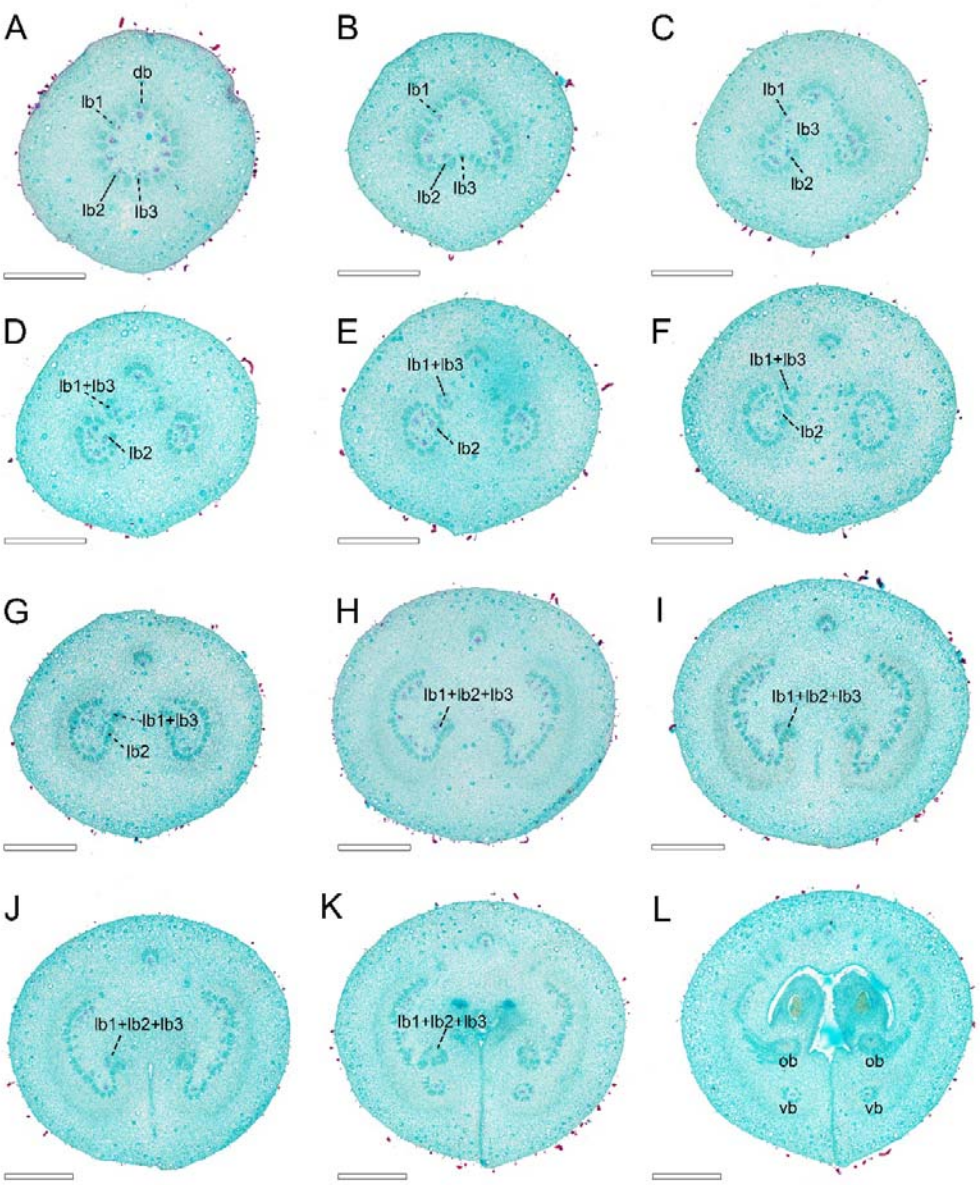

FIGURE 5. Ascending paraffin transections of mature *A. luzonensis* carpel. **(A)** Carpel base, showing basal ring. **(B–C)** Basal ring breaks on ventral side. **(D–F)** Ascending carpel stipe sections, showing lateral bundles reconstituted to two sets of ring-arranged lateral bundle complexes. **(G–H)** Top of carpel stipe, showing "C"-shaped lateral bundle complex. **(I–K)** Below ovary locule, showing formation of ovule bundles. **(L)** Base of ovary locule. db, dorsal bundle; lb, lateral bundle; vb, ventral bundle; ob, ovule bundle. Scale bars = 500 μm.

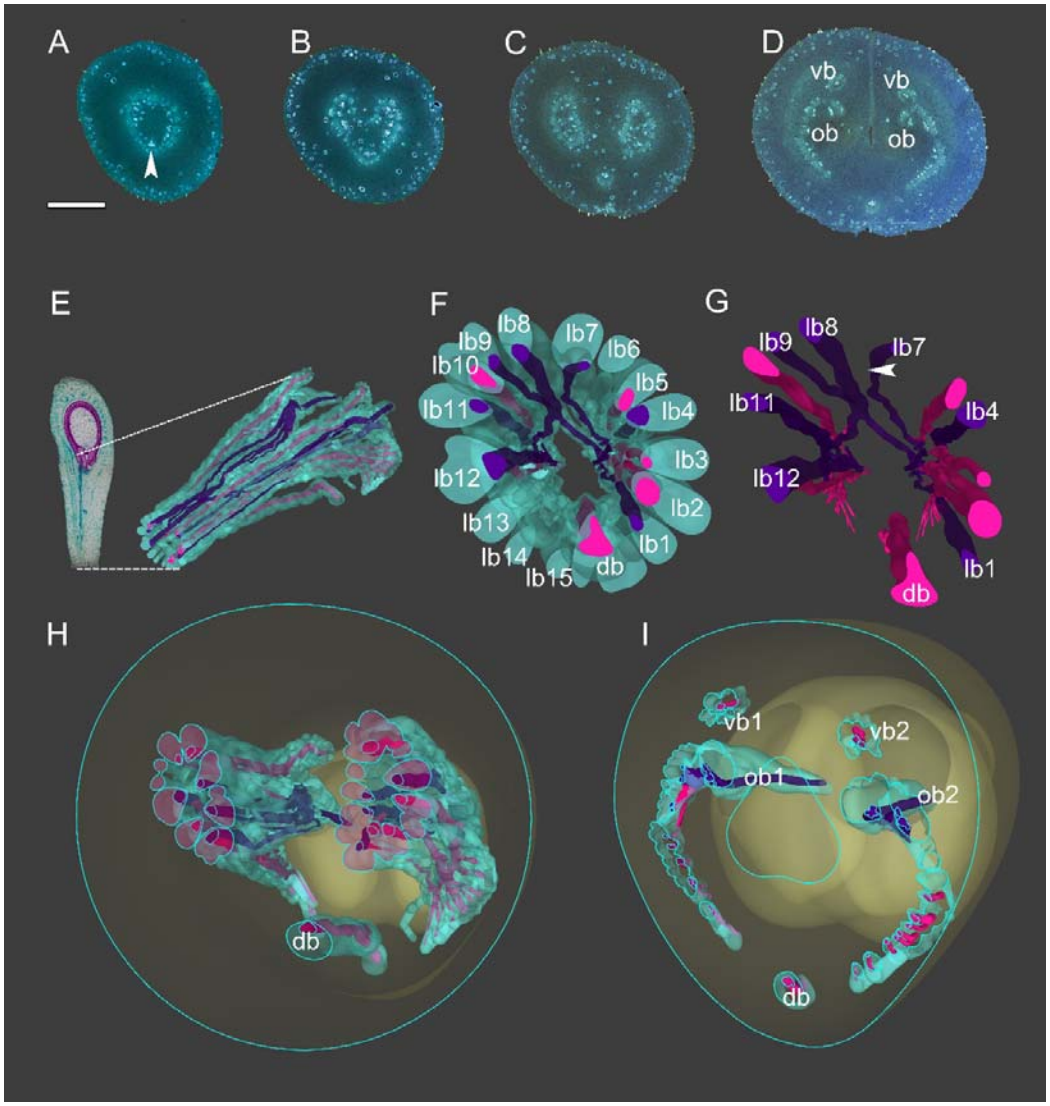

FIGURE 6. 3D construction of *A. javanica* vasculature.

Bundle outlines colored green, xylem red, and purple, among which bundles associated with ovule bundles are colored purple. **(A–D)** Aniline blue-stained *A. javanica* sections for modeling. **(E)** Longitudinal section of mature *A. javanica* carpel (left) and 3D vasculature model, dotted lines on longitudinal section indicate vasculature position in carpel. **(F)** Perspective from base of carpel vasculature. **(G)** Perspective from base of carpel (xylem only). The arrow indicates the intersection of two lateral bundles which fed two ovules respectively. **(H)** Cross-section of 3D model corresponding to **(C)**, showing ring-arranged lateral bundle complexes. **(I)** 3D model section showing distribution of vascular bundles at base of ovary. db, dorsal bundle; vb, ventral bundle; ob, ovule bundle, lb, lateral bundle. Scale bars = 500 μm.

DISCUSSION

In this study, 3D reconstruction was used to resolve the complex spatial relationship of carpel vasculature in *Anaxagorea*. In addition, this study is the first to report the basal ring and the ringed lateral bundle complex in the carpel. Observations on the continuous changes in vasculature from the receptacle to the carpel showed that the ringed vasculature pattern was topologically continuous and repeatedly presented in the pedicel, the receptacle, the base of the carpel, and the placenta.

Anaxagorea Carpel Organogenesis

Peltate carpels have been suggested to be plesiomorphic in Annonaceae (Deroin, 1988; Igersheim and Endress, 1997; Surveswaran et al., 2010; Couvreur et al., 2011) and in some studies, *Anaxagorea* carpels have been reported to exhibit an ascidiate base (Deroin, 1988), while they have been described as completely plicate in others (Endress and Armstrong, 2011). In this study, floral organogenesis revealed that the carpel stipe emerges from the base of *A. luzonensis* and *A. javanica* carpels in the early stages of carpel development and elongate with the development of the carpel. In the flowering stage, the ventral slit of *A. luzonensis* terminates close to the base of the ovary locule, resulting in a very short ascidiate zone, while in *A. javanica*, it may continue below the ovary locule. These variations might suggest a transformation from peltate to plicate carpels in this genus. The specific carpel stipe of *Anaxagorea* provides a buffer for the drastic changes in carpel base vasculature and makes it an ideal material for exploring the possible axial homologous structure in the carpel.

Anaxagorea Floral Vasculature

Previous studies have reported that the Annonaceae gynoecium is fed by an enlarged central stele, and each carpel is usually fed by three bundles, one median and two lateral (Deroin, 1989; De Craene, 1993; Deroin and Norman, 2016; Deroin and Bidault, 2017). However, in *A. luzonensis* and *A. javanica*, the number of vascular bundles that fed the carpel during anthesis is significantly more than three, regardless of the number of carpels, and the number of vascular bundles enter the *A. luzonensis* gynoecium is consistent with the central stele. The bundles entering the carpel are arranged in a radiosymmetric pattern, and this pattern maintains spatiotemporal continuity throughout the carpel stipe. Considering that radiosymmetric vasculature is a universal feature in vascular plant stems (Metcalfe and Chalk, 1979; Evert, 2006; Beck, 2010; McKown and Dengler, 2010; Evert and Eichhorn, 2011), it is plausible that the basal ring represents the homology of the carpel and the axial structures. In the basal ring, there are two lateral bundles which are fed to both ovules (lb8 and lb9 in **Figure 6G**), which makes the topological structure of the basal ring unable to be flattened into a leaf-like structure bearing marginal ovules.

It has been reported that in *Anaxagorea*, the ovules are served by the lateral bundle complex from the base of the carpel [e.g., *A. luzonensis* (Deroin, 1997); *A. crassipetala* (Endress, 2011)]. This pattern is different from that of most cases in Annonaceae, in which has ovules are served by separate vascular bundles branching directly from the dorsal bundles [e.g., *Cananga* (Deroin and Le Thomas, 1989);

Deeringothamnus (Deroin and Norman, 2016); and *Pseudartabotrys* (Deroin and Bidault, 2017)] or from relatively dorsally positioned bundles of the lateral network of bundles [e.g., *Meiocarpidium* (Deroin, 1987); and *Ambavia* (Deroin and Le Thomas, 1989)]. Our study showed that the topological structure of the ring-arranged lateral bundle complexes plays a key role in forming the ovule bundles and that it facilitates the non-adjacent bundles to approach each other and merge. The dorsal bundle remained independent throughout, and there were no horizontal connections between dorsal bundle and the lateral bundle complexes. The ventral bundle participated in the formation of the spatial ring- arrangement of the lateral bundle complexes; however, it was not involved in forming of ovule bundles. The stimulus for vascular bundle formation comes from the base of the leaf primordium. After primordium formation, auxin sinks down into the inner tissue, thereby defining the course of subsequently differentiated vascular bundle (Runions et al., 2014). According to the hypothesis that the placenta or ovule may originate from the bracteole-terminal ovule system of female secondary reproductive branch, it is essential to explore whether the ring-arranged lateral bundle complexes are related to ovule organogenesis. Another important distinction between *Anaxagorea* and other genera of Annonaceae is that *Anaxagorea* exhibits explosive dehiscence of fruits; therefore, the ring-shaped lateral bundle complex may also be associated with that feature.

Observation of the different developmental stages of the *Anaxagorea* carpel showed that the amphicribral bundle complexes in the placenta developed into the ring-arranged lateral bundle complexes with carpel maturation. The ovule bundles are also amphicribral. In the vasculature development, the amphicribral bundles could be discrete inversely collateral bundles near the point of fusion, because their xylem portions need to approach each other before they become concentric (Endress, 2019). Based on derivation, the amphicribral bundles are frequently observed in small branches of early land plants, monocots, or immature young branches of dicots (Fahn, 1990). If the carpels are indeed derived from the integrated axial-foliar complex, it could explain why the amphicribral bundles are widespread in angiosperm placentae and funiculi [e.g., *Papaver* (Kapoor, 1973); *Psoraleae* (Lersten and Don, 1966); *Drimys* (Tucker, 1975); *Nicotiana* (Dave et al., 1981); *Whytockia* (Wang and Pan, 1998); *Pachysandra* (Von Balthazar and Endress, 2002); *Magnolia* (Liu et al., 2014); *Michelia* (Zhang et al., 2017); *Actinidia* (Guo et al., 2013); and *Dianthus* (Guo et al., 2017)]. However, this does not imply that the amphicribral bundle can be used to determine the type of organ from which it was formed because the histology of a vascular bundle is greatly influenced by the subsequent older vascular bundle to which it connects (Endress, 2019).

In *Anaxagorea*, the central stele, basal ring, ringed lateral bundle complex, and amphicribral ovule bundle exhibit similar topological properties, which supports the view that the carpel is the product of fusion between an ovule-bearing axis and the phyllome that subtends it. The composite origin of carpels facilitates the understanding of the composite origin of ovules, i.e., determining how the bract-bracteole-terminal ovule system in angiosperm precursors evolved into an angiosperm carpel. However, the homology comparison based on vasculature has

366 some limitations. The underlying signals regulating vasculature are not yet fully
367 understood. Technologies that are capable of simultaneously providing functional,
368 physiological, and anatomical information, such as Magnetic Resonance Imaging and
369 the visualization of molecular processes, could help facilitate future research.

AUTHOR CONTRIBUTIONS

YL planned and designed the research, performed the experiments, collected the images, drew the illustrations, and wrote the article; WD performed the experiments and complemented the writing; YC developed the 3D model; SW complemented the writing; X-FW supervised the experiments and complemented the writing.

FUNDING

This study was supported by the National Natural Science Foundation of China (grant number 31270282, 31970250).

ACKNOWLEDGMENTS

We thank Profs. Lars Chatrou, Xin Wang, and Xin Zhang for their helpful suggestions to the manuscript. We also thank Chun-Hui Wang, Shi-Rui Gan, and Yan-Lian Qiu for their help in searching for the target species in the field, Qing-Long Wang for his assistance in caring for the transplant materials in Hainan province, Qiang Liu for his support during sampling, and Lan-Jie Huang and Ke Li for their advice on manuscript writing. We would also like to thank Editage for English language editing.

REFERENCES

Angenent, G. C., Franken, J., Busscher, M., van Dijken, A., van Went, J. L., Dons, H. J., and van Tunen, A. J. (1995). A novel class of MADS box genes is involved in ovule development in *Petunia*. *Plant Cell* 7, 1569–1582. doi: 10.2307/3870020

Beck, C. B. (2010). *An Introduction to Plant Structure and Development: Plant Anatomy for the Twenty-first Century*, 2nd edn. Cambridge, New York: Cambridge University Press.

Chatrou, L. W., Pirie, M. D., Erkens, R. H. J. , Couvreur, T. L. P., Neubig, K.M., Abbott, J. R., et al. (2012). A new subfamilial and tribal classification of the pantropical flowering plant family Annonaceae informed by molecular phylogenetics. *Bot. J. Linn. Soc.* 169, 5–40. doi:10.1111/j.1095-8339.2012.01235.x

Chatrou, L. W., Turner, I. M., Klitgaard, B. B, Maas, P. J. M., and Utteridge, T. M. A. (2018). A linear sequence to facilitate curation of herbarium specimens of Annonaceae. *Kew Bull.* 73:39. doi: 10.1007/S12225-018-9764-3

Dave, Y. S., Patel, N. D., and Rao, K. S. (1981). Structural design of the developing fruit of *Nicotiana tabacum*. *Phyton* 21, 63–71.

De Craene, L. P. R., and Smets, E. F. (1993). The distribution and systematic relevance of the androecial character polymery. *Bot. J. Linn. Soc.* 113, 285–350. doi: 10.1111/j.1095-8339.1993.tb00341.x

Deroin, T. (1988). *Aspects anatomiques et biologiques de la fleur des Annonacées*. [PhD thesis]. [Centre d'Orsay (France)]: Université de Paris-Sud.

Deroin, T. (1989). Définition et signification phylogénique des systèmes corticaux floraux: l'exemple des Annonacées. *Comptes Rendus de l'Académie des Sciences, Paris* 308, Série III, 71–75.

Deroin, T., and Le Thomas, A. (1989). "Sur la systématique et les potentialités évolutives des Annonacées: cas d'*Ambavia gerrardii*," in *Espèce Endémique de Madagascar*, Série III. ed. A. le Thomas. (*Comptes Rendus de l'Académie des Sciences Paris*) 309: 647–652.

Deroin, T. (1997). Confirmation and origin of the paracarpy in Annonaceae, with comments on some methodological aspects. *Candollea* 52: 45–58.

Deroin, T, and Norman, É. M. (2016). Notes on the floral anatomy of *Deeringothamnus* Small (Annonaceae): cortical vascular systems in a chaotic pattern. *Modern Phytomorphology* 9, 3–12.

Deroin, T., and Bidault, E. (2017). Floral anatomy of *Pseudartabotrys* Pellegrin (Annonaceae), a monospecific genus endemic to Gabon. *Adansonia* 39, 111–123. doi: 10.5252/a2017n2a2

Doyle, J. A., and Le Thomas, A. (1996). Phylogenetic analysis and character evolution in Annonaceae. *Adansonia* 18, 279–334.

Doyle, J. A., Sauquet, H., Scharaschkin, T., and Le Thomas, A. (2004). Phylogeny, molecular and fossil dating, and biogeographic history of Annonaceae and Myristicaceae (Magnoliales). *Int. J. Plant Sci.* 165, S55–S67. doi: 10.1086/421068

Doyle, J. A. (2008). Integrating molecular phylogenetic and paleobotanical evidence on origin of the flower. *Int. J. Plant Sci.* 169, 816–843. doi: 10.1086/589887

Dunal, M. F. (1817). Monographie de la famille des Anonacées. Paris: Treuttel & Würtz.

Endress, P. K., Armstrong, J. E. (2011). Floral development and floral phyllotaxis in *Anaxagorea* (Annonaceae). *Ann. Bot.* 108, 835–845. doi: 10.1093/aob/mcr201

Endress, P. K. (2005). Carpels in *Brasenia* (Cabombaceae) are Completely Ascidiate

437 Despite a Long Stigmatic Crest. *Ann. Bot.* 96, 209–215. doi: 10.1093/aob/mci174
438 Endress, P. K. (2015). Patterns of angiospermy development before carpel sealing
439 across living angiosperms: diversity, and morphological and systematic aspects. *Bot.*
440 *J. Linn. Soc.* 178, 556–591. doi: 10.1111/boj.12294
441 Endress, P. K. (2019). The morphological relationship between carpels and ovules in
442 angiosperms: pitfalls of morphological interpretation. *Bot. J. Linn. Soc.*189,
443 201–227. doi: 10.1093/botlinnean/boy083
444 Evert, R. F., and Eichhorn, S. E. (2013). *Raven Biology of Plants,* 8th edn. Palgrave
445 Macmillan: W.H. Freeman Press.
446 Evert, R. F. (2006). *Esau's Plant Anatomy. Meristems, Cells, and Tissues of the Plant*
447 *Body: Their Structure, Function, and Development,* 3rd edn. Hoboken, NJ: John
448 Wiley & Sons, Inc.
449 Guo, X. M., Xiao, X., Wang, G. X., and Gao, R. F. (2013). Vascular anatomy of kiwi
450 fruit and its implications for the origin of carpels. *Front. Plant Sci.* 4: 391. doi:
451 10.3389/fpls.2013.00391
452 Guo, X. M., Yu, Y. Y., Bai, L., and Gao, R. F. (2017). *Dianthus chinensis* L.: the
453 structural difference between vascular bundles in the placenta and ovary wall
454 suggests their different origin. *Front. Plant Sci.* 8: 1986. doi:
455 10.3389/fpls.2017.01986
456 Kapoor, L. D. (1973). Constitution of amphicribral vascular bundles in capsule of
457 *Papaver somniferum*. Linn. *Botanical Gazette* 134, 161–165. doi: 10.1086/336698
458 Kaul, R. B. (1967). Development and vasculature of the flowers of *Lophotocarpus*
459 *calycinus* and *Sagittaria latifolia* (Alismaceae). *Am. J. Bot.* 54, 914–920. doi:
460 10.1002/j.1537-2197.1967.tb10715.x
461 Kennedy, D., and Norman, C. (2005) What don't we know? *Science* 309, 78–102. doi:
462 10.1126/science.309.5731.75
463 Lersten, N. R., and Don, K. W. (1966). The discontinuity plate, a definitive floral
464 characteristic of the *Psoraleae* (Leguminosae). *Am. J. Bot.* 53, 548–555. doi:
465 10.2307/2440004
466 Liu, W. Z., Hilu, K., and Wang, Y. L. (2014). From leaf and branch into a flower:
467 *Magnolia* tells the story. *Bot. Stud.* 55: 28. doi: 10.1186/1999-3110-55-28 doi:
468 10.1186/1999-3110-55-28
469 Magallon, S., Gomez-Acevedo, S., Sanchez-Reyes, L. L., et al. (2015). A
470 metacalibrated time-tree documents the early rise of flowering plant phylogenetic
471 diversity. *New phytol.* 207: 437–453 doi: 10.1111/nph.13264
472 Mathews, S. and Kramer, E. M. (2012). The Evolution of Reproductive Structures in
473 Seed Plants: A Re-Examination Based on Insights from Developmental Genetics.
474 *New phytol.*194, 910–923. doi: 10.1111/j.1469-8137.2012.04091.x
475 McKown, A. D., and Dengler, N. G. (2010). Vein patterning and evolution in C4 plants.
476 *Botany* 88, 775–786. doi: 10.1139/B10-055
477 Metcalfe, C. R., and Chalk, L. (1979). *Anatomy of the Dicotyledons, vol. 1, Systematic*
478 *Anatomy of Leaf and Stem, with a Brief History of the Subject,* 2nd edn. Oxford:
479 Clarendon Press.
480 Robertson, R. E., and Tucker, S. C. (1979). Floral ontogeny of *Illicium floridanum*,
481 with emphasis on stamen and carpel development. *Am. J. Bot.* 66, 605–617. doi:
482 10.1002/j.1537-2197.1979.tb06264.x
483 Robinson-Beers, K., Pruitt, R. E., and Gasser, C. S. (1992). Ovule development in
484 wild-type Arabidopsis and two female-sterile mutants. *Plant Cell* 4, 1237–1249.

485 doi: 10.1105/tpc.4.10.1237
486 Runions, A., Smith, R. S., and Prusinkiewicz, P. (2014). "Computational models of
487 auxin-driven development," in *Auxin and its Role in Plant Development*, eds.
488 Zažímalová, E., Petrášek, and J., Benková, E (Vienna: Springer), 315–357.
489 Sauquet, H., Doyle, J. A., Scharaschkin, T., Borsch, T., Hilu, K. W., Chatrou, L. W.,
490 et al. (2003). Phylogenetic analysis of Magnoliales and Myristicaceae based on
491 multiple data sets: implications for character evolution. *Bot. J. Linn. Soc.* 142,
492 125–186. doi: 10.1046/j.1095-8339.2003.00171.x
493 Skinner, D. J., Hill, T. A., Gasser, C. S. (2004). Regulation of Ovule Development.
494 *Plant Cell* 16, S32–S45. doi: 10.1105/tpc.015933
495 Soltis, P. S., Soltis, D. E., Savolainen, V., Crane, P. R., and Barraclough, T. G. (2002).
496 Rate heterogeneity among lineages of tracheophytes: Integration of molecular and
497 fossil data and evidence for molecular living fossils. *P. Natl. Acad. Sci. USA* 99,
498 4430–4435. doi:10.1073/pnas.032087199
499 Tucker, S. C. (1975). Carpellary vasculature and the ovular vascular supply in *Drimys*.
500 *Am. J. Bot.* 62, 191–197. doi: 10.1002/j.1537-2197.1975.tb14052.x
501 Tucker, S. C. (1961). Phyllotaxis and vascular organization of the carpels in *Michelia*
502 *fuscata*. *Am. J. Bot.* 48, 60–71. doi: 10.1002/j.1537-2197.1961.tb11605.x
503 Von Balthazar, M., and Endress, P. K. (2002). Reproductive structures and systematics
504 of Buxaceae. *Bot. J. Linn. Soc.* 140, 193–228. doi:
505 10.1046/j.1095-8339.2002.00107.x
506 Wang, X. (2010). *The dawn angiosperms*. Heidelberg: Springer.
507 Wang, X. (2018). *The dawn angiosperms*, 2nd edn. Heidelberg: Springer.
508 Wang, Y. Z., and Pan, K. Y. (1998). "Comparative floral anatomy of Whytockia
509 (Gesneriaceae) endemic to China," in *Floristic Characteristics and Diversity of*
510 *East Asian Plants*, eds. A. L. Zhang, and S. G. Wu (Beijing: China Higher
511 Education Press), 352–366.
512 Winter, K. U., Becker, A., Münster T., Kim, J. T., Saedler, H., and Theissen, G. (1999).
513 MADS-box genes reveal that gnetophytes are more closely related to conifers than
514 to flowering plants. *P. Natl. Acad. Sci USA* .96, 7342–7347 doi:
515 10.1073/pnas.96.13.7342
516 Wynn, A. N., Seaman, A. A., Jones, A. L., and Franks R. G. (2014). Novel functional
517 roles for PERIANTHIA and SEUSS during floral organ identity specification,
518 floral meristem termination, and gynoecial development. *Front. Plant Sci.* 5: 130.
519 doi: 10.3389/fpls.2014.00130
520 Zhang, X., Liu, W., and Wang, X. (2017). How the ovules get enclosed in
521 magnoliaceous carpels. *PLoS One* 12: e0174955.
522 doi:10.1371/journal.pone.0174955
523 Zhang, X., zhang, Z. X. and Zhao, Z. (2019). Floral ontogeny of *Illicium Lanceolatum*
524 (Schisandraceae) and its implications on carpel homology. *phytotaxa* 416, 200–210.
525 doi: 10.11646/phytotaxa.416.3.1